A New Iterative Procedure for the Localization of a Moving Object/Person in Indoor Areas from Received RF Signals

Rym Hicheri
Faculty of Engineering and Science
University of Agder
NO-4898 Grimstad, Norway
rym.hicheri@uia.no

Matthias Pätzold
Faculty of Engineering and Science
University of Agder
NO-4898 Grimstad, Norway
matthias.paetzold@uia.no

***Abstract*—This paper presents a new iterative estimation method to localize a single moving object or person in non-stationary 3-dimensional (3D) indoor environments from received radiofrequency (RF) signals. The moving object/person is modelled by a moving single point scatterer. The indoor space is equipped with a multiple-input multiple-output (MIMO) communication system. This work starts by introducing a new geometrical channel model which considers the effects of the line-of-sight (LOS) component, the fixed objects located in a room, and the moving object (point scatterer). Then, we present an iterative estimation technique for computing the time-variant (TV) coordinates of the moving scatterer. The proposed approach determines the optimal TV coordinates of the moving scatterer by matching the TV transfer function (TVTF) of the received RF signals to the TVTF of the non-stationary channel model. The proposed procedure relies on numerical optimization techniques to estimate the TV position of the moving scatterer by minimizing the Euclidean norm of the fitting error. A comparison of the estimated TV position of the moving scatterer with the corresponding exact quantities, known from generated RF signals, confirms the validity of the proposed approach.**

I. Introduction

Owing to their wide range of applications, there is currently a high demand for precise techniques for locating moving (non-stationary) objects or persons in indoor areas, e.g., [1], [2].

Although several popular and successful solutions have been developed in the context of outdoor mobile-radio applications (GPS, Galileo, Glonass, and BeiDou) [3], they cannot be applied to indoor environments, in which signals experience attenuation, rich scattering, and multipath propagation phenomena [2], [4].

Examples of existing approaches for indoor location, such as infra-red light, ultra-wideband, and computer vision, can be found in [2]. As discussed in [2], [5], [6], the performance of these techniques is sensitive to the complexity of human movements in crowded (very furnished) indoor environments. Wi-Fi-based methods have established themselves as promising indoor localization solutions due to their worldwide distribution, simplicity of infrastructure, and financial advantages. Indoor position estimators utilizing Wi-Fi technology can be classified according to the methods they employ; received signal strength indicator-based techniques, time-of-arrival-based procedures, angle-of-arrival (AOA)-based methods, and the fingerprinting-based algorithms [2], [4], [7]–[10]. With the increasing use of stationary cameras in indoor areas and the popularity and affordability of mobile devices (e.g., smartphones, smartwatches, tablets, etc.) equipped with a variety of hardware sensors (accelerometers, gyroscopes, and magnetometers), heterogeneous designs of RF systems for indoor positioning with data (image, video, multi-sensor data fusion) analysis have also been investigated [11]. As mentioned in [2], [5], and [6], the precision and accuracy of Wi-Fi-based localization methods is significantly affected by: the high presence of solid objects in indoor spaces (walls, ceilings, decorative objects, furniture), the attenuation of the received RF signals (due to diffraction, reflection, and refraction), the multipath propagation, and the strength of the line-of-sight (LOS) signal.

To contribute to the topic of indoor positioning, we propose a new iterative method to estimate the time-variant (TV) position of a single moving object or person in three-dimensional (3D) indoor environments from the received RF signals. In this work, we consider the effects of rich scattering (resulting from the fixed objects in the room) as well as the presence of the LOS components. Although several channel parameter estimators have been proposed [12]–[16], they employ the frequency or time-frequency correlation function, consider stationary scenarios (constant speed), and mainly investigate the Doppler frequencies, AOA, constant path gains and paths delays. In the context of non-stationary indoor channels, iterative techniques have been presented to estimate the TV velocity of a moving object/person from the Doppler characteristics (spectrogram) of the complex channel gain [17], [18], because a small variation of the TV position of a moving object cannot be visualized in the spectrogram. Although these methods compute the channel parameters, it is difficult to retrieve the TV position of a moving

object/person.

Inspired by [15] and [16], we present a new iterative procedure to estimate the position of a single moving object/person (modelled by a single point moving scatterer) using the TV transfer function (TVTF), considering non-stationary scenarios (TV position and TV speed), TV path gains, and TV path delays. First, we introduce a new 3D non-stationary MIMO channel model with TV path gains and TV path delays. Then, the proposed positioning procedure determines the optimal TV position of the moving object/person by fitting the TVTF of the received signal to the TVTF of the channel model. The estimated quantities are obtained through numerical optimization by minimizing the Euclidean norm of the fitting error. A good match between the exact coordinates of the moving scatterer, known from test RF signals generated by means of computer simulations, and their estimates confirms the validity and accuracy of the proposed algorithm. Numerical results show that the proposed positioning algorithm allows an accurate localization of the moving object/person with an average Euclidean error of approximately 6 cm and 10.5 cm when employing 3×3 and 2×2 MIMO systems, respectively.

The paper is organized as follows. Section II describes the investigated scenarios. A new 3D channel model and its features are introduced in Section III. The proposed iterative estimation method is the subject of Section IV. Finally, Section V concludes the paper.

II. Scenario Description

In this section, we review the channel model employed to describe the propagation scenario in the 3D indoor space. As illustrated in Fig. 1, we consider a typical room with length A, width B, and height H. The room is equipped with a MIMO communication system. Both the transmitter T_X and the receiver R_X are equipped with N_T and N_R antenna elements A_j^T $(j = 1, 2, \ldots, N_T)$ and A_i^R $(i = 1, 2, \ldots, N_R)$, respectively. As shown in Fig. 1, there are several stationary (fixed) objects in the room such as walls, furniture, and decoration items. In addition, there is a moving object/person (★). The moving person/object is modelled by a single moving point scatterer which represents the centre of gravity of the person/object.

The propagation phenomenon is modelled by means of the 3D geometrical channel model shown in Fig. 2. The jth transmit antenna A_j^T is located at the coordinates (x_j^T, y_j^T, z_j^T), $j = 1, 2, \ldots, N_T$. Analogously, the ith receive antenna A_i^R is located at the position (x_i^R, y_i^R, z_i^R), $i = 1, 2, \ldots, N_R$. The fixed objects in the room, which are seen between A_i^T and A_j^R, are modelled by K_{ij} fixed scatterers $S_{k_{ij}}^F$, $k_{ij} = 1, 2, \ldots, K_{ij}$, which are represented by the symbol (•). On the other hand, the single moving object or person in the room is modelled by a single point moving scatterer S^M, which is represented by the symbol (★). The point scatterer S^M corresponds to the center of mass (center of gravity) of the moving object/person and has the TV coordinates $(x(t), y(t), z(t))$. As shown in Fig. 2, the quantity $D_j^T(t)$ $(j = 1, 2, \ldots, N_T)$ represents the distance between the jth transmit antenna element A_j^T and the scatterer S^M, while the parameter $D_i^R(t)$ $(i = 1, 2, \ldots, N_R)$ refers to the distances between the ith receive antenna element A_i^R and the scatterer S^M. In the following, we take into account the presence of a LOS component and consider single-bounce scattering when modelling the multipath components due to the stationary (fixed) scatterers. It should be mentioned that, in the following, all parameters (number and positions) related to the the T_X and R_X antenna elements are assumed to be known.

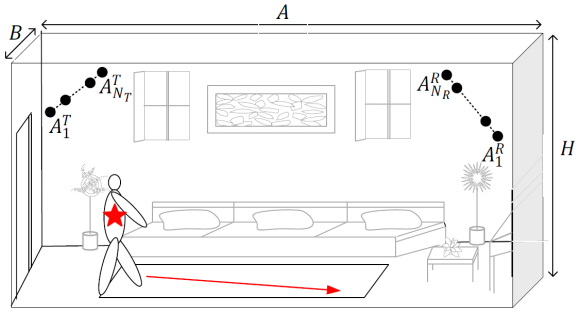

Fig. 1. A typical room architecture with the MIMO communication system and the stationary objects [18, Fig. 1].

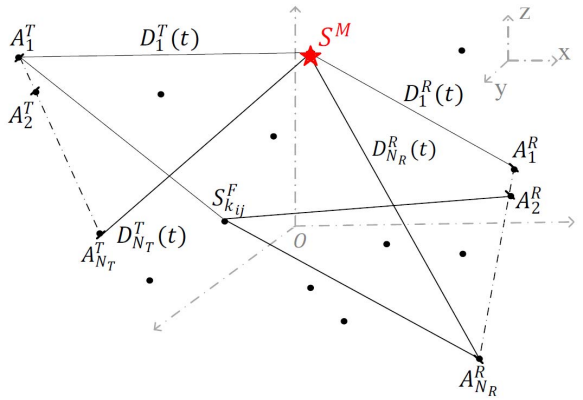

Fig. 2. The 3D geometrical model for an $N_T \times N_R$ MIMO channel with fixed and moving scatterers.

III. The Channel Model

This section describes the analytical 3D non-stationary channel model that will later be used to estimate the position as well as the speed of the moving object or person (scatterer). We consider an indoor environment equipped with an $N_T \times N_R$ MIMO communication system. According to Fig. 2, the TVTF $H_{ij}(f', t)$ of the indoor channel between the jth transmit antenna

A_j^T and ith receive antenna A_i^R can be expressed as

$$H_{ij}(f',t) = c_{ij}(t)\exp\left(j\left(\theta_{ij} - 2\pi f'\tau'_{ij}(t)\right)\right) + \sum_{k_{ij}=0}^{K_{ij}} c_{k_{ij}}\exp\left(j\left(\theta_{k_{ij}} - 2\pi f'\tau'_{k_{ij}}\right)\right) \quad (1)$$

where the first term describes the impact of the moving object and the second term represents the multipath component resulting from the fixed scatterers (objects in the room). In (1), the quantities $c_{ij}(t)$ and $\tau'_{ij}(t)$ refer to the TV path gain and TV delay given by $c_{ij} = CD_{ij}(t)^{-\gamma}$ and $\tau'_{ij}(t) = D_{ij}(t)/c_0$, respectively. Here, C is a constant which depends on the transmit/receive antenna gain, the transmission power as well as the wavelength [19], [20], γ is the path loss exponent, which depends on the propagation environment, and c_0 is the speed of light. With reference to Fig. 2, the total distance $D_{ij}(t) = D_j^T(t) + D_i^R(t)$ is given by

$$D_{ij}(t) = \left[\left(x(t)-x_j^T\right)^2 + \left(y(t)-y_j^T\right)^2 + \left(z(t)-z_j^T\right)^2\right]^{1/2} + \left[\left(x_i^R-x(t)\right)^2 + \left(y_i^R-y(t)\right)^2 + \left(z_i^R-z(t)\right)^2\right]^{1/2}. \quad (2)$$

The initial phases θ_{ij} of the channel are modelled by independent and identically distributed (i.i.d.) random variables, each having a uniform distribution over the interval $[0, 2\pi)$. Note that the TV delays $\tau'_{ij}(t)$ describe the Doppler effect resulting from the single moving person or object by means of the fundamental relationship connecting the TV delays $\tau'_{ij}(t)$ and the TV Doppler frequencies $f_{ij}(t)$ as presented in [21]. Although the result in [21] has been reported in the context of a fixed transmitter T_X, a moving receiver R_X, and fixed scatterers, it can be easily shown that the relationship remains valid for the scenario investigated in this paper. Thus, the estimation of the TV position $(x(t), y(t), z(t))$ allows the determination of the TV Doppler frequencies $f_{ij}(t)$ according to [22].

Moreover, the quantities $c_{k_{ij}}$ and $\tau'_{k_{ij}}$ denote the path gain and delay of the k_{ij}th fixed scatterer $S_{k_{ij}}^F$ for $k_{ij} = 1, 2, \ldots, K_{ij}$. Since the LOS component does not experience any Doppler shift, it can be modelled as the fixed scatterer S_0^F ($k_{ij} = 0$). The phases $\theta_{k_{ij}}$ are i.i.d. random variables uniformly distributed over the interval $[0, 2\pi)$. In this work, our main objective is to estimate the TV position of the moving scatterer (object or person) S_M. Therefore, the overall effect of the fixed scatterers, represented by the second term of (1), can be replaced by a single complex term $c_{ijF}(f')\exp[j(\vartheta_{ijF}(f'))]$, where the gain $c_{ijF}(f')$ and phase $\vartheta_{ijF}(f')$ are given by $c_{ijF}(f') = \{[\sum_{k_{ij}=0}^{K_{ij}} c_{k_{ij}}\cos(\theta_{k_{ij}} - 2\pi f'\tau'_{k_{ij}})]^2 + [\sum_{k_{ij}=0}^{K_{ij}} c_{k_{ij}}\sin(\theta_{k_{ij}} - 2\pi f'\tau'_{k_{ij}})]^2\}^{1/2}$ and $\vartheta_{ijF}(f')$=atan2$(\sum_{k_{ij}=0}^{K_{ij}} c_{k_{ij}}\sin(\theta_{k_{ij}} - 2\pi f'\tau'_{k_{ij}}), \sum_{k_{ij}=0}^{K_{ij}} c_{k_{ij}}\cos(\theta_{k_{ij}} - 2\pi f'\tau'_{k_{ij}}))$, respectively. Here, atan2 refers to the inverse tangent function which returns the angle between $-\pi$ and π, unlike the traditional $\arctan$ function which returns the angle between $-\pi/2$ and $\pi/2$.

In reality, the TVTF $\hat{H}_{ij}(f'_q, t_p)$ of the received RF signal is computed from measured samples of the channel at discrete time instances $t_p = p\Delta t \in [0, T]$, $p = 0, \ldots, P-1$, and discrete frequencies $f'_q = -B/2 + q\Delta f' \in [-B/2, B/2]$, $q = 0, \ldots, Q-1$, in which T and B are the total observation time interval and the measured frequency bandwidth. The time sampling Δt and the frequency sampling period $\Delta f'$ are characteristic parameters of the channel sounder employed to collect the RF data.

The main purpose of this paper is to propose a new iterative procedure to estimate the TV position a moving object/person. The description of this estimation method will be the topic of the next section.

IV. The Estimation Algorithm

The problem at hand, is to determine, at each time instant t_p, the position $(x_p, y_p, z_p) = (x(t_p), y(t_p), z(t_p))$ of the moving object (scatterer) S^M in the indoor area, the propagation parameter γ, and the parameter C. First, we determine, at each time instant t_p, a set of parameters $\mathcal{P}_{t_p} = \{x_p, y_p, z_p, C, \gamma, \theta_{ij0}\}$ by fitting the complex channel gains $H_{ij}(f'_q, t_p)$ of the geometrical channel model as close as possible to the TVTF $\hat{H}_{ij}(f'_q, t_p)$ of the received RF signals, i.e.,

$$\mathcal{P}_{t_p} = \underset{\mathcal{P}_{t_p}}{\operatorname{argmin}} \sum_{q=0}^{Q-1}\sum_{j=1}^{N_T}\sum_{i=1}^{N_R}\left|\hat{H}_{ij}(f'_q, t_p) - H_{ij}(f'_q, t_p)\right|^2. \quad (3)$$

In order to compute the parameters of interest, we introduce the objective function $E(\mathcal{P}_{t_p})$ as

$$E(\mathcal{P}_{t_p}) = \sum_{q=0}^{Q-1}\sum_{j=1}^{N_T}\sum_{i=1}^{N_R}\left|\hat{H}_{ij}(f'_q, t_p) - H_{ij}(f'_q, t_p)\right|^2. \quad (4)$$

The set of parameters $\mathcal{P}_{t_p}$ is determined by minimizing the objective function in (4).

We start by arbitrary choosing the initial values of $x_p^{(0)}$, $y_p^{(0)}$, $z_p^{(0)}$, $C^{(0)}$, $\gamma^{(0)}$, and $\theta_{ij0}^{(0)}$. Then, we compute the new estimates of the parameters $x_p^{(l+1)}$, $y_p^{(l+1)}$, $z_p^{(l+1)}$, $v_p^{(l+1)}$, $C^{(l+1)}$, $\gamma^{(l+1)}$, and $\theta_{ij0}^{(l+1)}$ at every iteration l, $l = 0, 1, 2, \ldots$, according to the following optimization problem in (5) [see the top of the next page], in which $D_{ijp}(x_p, y_p, z_p) = D_{ij}(t_p)$ corresponds to the TV distance $D_{ij}(t)$ evaluated at the time instant t_p, and expressed in terms of the TV coordinates x_p, y_p, and z_p of the moving scatterer (object or person) S_M. The proposed estimation technique works as follows. First, we compute the new estimate of $x_p^{(l+1)}$ that is a global minimum of the right-hand side of (5). Then, by utilizing $x_p^{(l+1)}$, the optimization problem in (5),

$$\left(x_p^{(l+1)}, y_p^{(l+1)}, z_p^{(l+1)}, C^{(l+1)}, \gamma^{(l+1)}, \theta_{ij}^{(l+1)}\right) = \underset{\mathcal{P}_{t_p}}{\operatorname{argmin}} \sum_{q=0}^{Q-1} \sum_{j=1}^{N_T} \sum_{i=1}^{N_R} \left| \hat{H}_{ij}(f'_q, t_p) - \; c_{ij}^F\left(f'_q\right) \exp\left(-j\vartheta_{ij}^F\left(f'_q\right)\right) - \frac{C}{D_{ijp}^{\gamma}(x_p, y_p, z_p)} \exp\left(j\left(\theta_{ij} - 2\pi f'_q \frac{D_{ijp}(x_p, y_p, z_p)}{c_0}\right)\right) \right|^2 . \quad (5)$$

$$\left(y_p^{(l+1)}, z_p^{(l+1)}, C^{(l+1)}, \gamma^{(l+1)}, \theta_{ij}^{(l+1)}\right) = \underset{\mathcal{P}_{t_p}\setminus\{x_p\}}{\operatorname{argmin}} \sum_{q=0}^{Q-1} \sum_{j=1}^{N_T} \sum_{i=1}^{N_R} \left| \hat{H}_{ij}(f'_q, t_p) - \; c_{ij}^F\left(f'_q\right) \exp\left(-j\vartheta_{ij}^F\left(f'_q\right)\right) - \frac{C}{D_{ijp}^{\gamma}\left(x_p^{(l+1)}, y_p, z_p\right)} \exp\left(j\left(\theta_{ij} - 2\pi f'_q \frac{D_{ijp}\left(x_p^{(l+1)}, y_p, z_p\right)}{c_0}\right)\right) \right|^2 . \quad (6)$$

$$\left(z_p^{(l+1)}, C^{(l+1)}, \gamma^{(l+1)}, \theta_{ij}^{(l+1)}\right) = \underset{\mathcal{P}_{t_p}\setminus\{x_p, y_p\}}{\operatorname{argmin}} \sum_{q=0}^{Q-1} \sum_{j=1}^{N_T} \sum_{i=1}^{N_R} \left| \hat{H}_{ij}(f'_q, t_p) - \; c_{ij}^F\left(f'_q\right) \exp\left(-j\vartheta_{ij}^F\left(f'_q\right)\right) - \frac{C}{D_{ijp}^{\gamma}\left(x_p^{(l+1)}, y_p^{(l+1)}, z_p\right)} \exp\left(j\left(\theta_{ij} - 2\pi f'_q \frac{D_{ijp}\left(x_p^{(l+1)}, y_p^{(l+1)}, z_p\right)}{c_0}\right)\right) \right|^2 . \quad (7)$$

$$\left(C^{(l+1)}, \gamma^{(l+1)}, \theta_{ij}^{(l+1)}\right) = \underset{\mathcal{P}_{t_p}\setminus\{x_p, y_p, z_p\}}{\operatorname{argmin}} \sum_{q=0}^{Q-1} \sum_{j=1}^{N_T} \sum_{i=1}^{N_R} \left| \hat{H}_{ij}(f'_q, t_p) - \; c_{ij}^F\left(f'_q\right) \exp\left(-j\vartheta_{ij}^F\left(f'_q\right)\right) - \frac{C}{D_{ijp}^{\gamma}\left(x_p^{(l+1)}, y_p^{(l+1)}, z_p(l+1)\right)} \exp\left(j\left(\theta_{ij} - 2\pi f'_q \frac{D_{ijp}\left(x_p^{(l+1)}, y_p^{(l+1)}, z_p(l+1)\right)}{c_0}\right)\right) \right|^2 . \quad (8)$$

reduces to that in (6) [see the top of this page]. The new estimate of $y_p^{(l+1)}$ is obtained in a similar manner, which yields the problem in (7) [see the top of this page]. Now, the updated estimate of $z_p^{(l+1)}$ corresponds to the value of z_p that minimizes the right-hand side of (7) [see the top of this page]. Finally, replacing the new value of $z_p^{(l+1)}$ in (7) results in the 3D optimization problem in (8) [see the top of this page]. The estimated values of $C^{(l+1)}$, $\gamma^{(l+1)}$, and $\theta_{ij}^{(l+1)}$ are determined from (8) by means of numerical computations.

The estimation steps in (5)−(8) are repeated as long as the relative error in the objective function is smaller than a predefined error value ε_1, i.e., $|E^{(l+1)}(\mathcal{P}_{t_p}) - E^{(l)}(\mathcal{P}_{t_p})| < \varepsilon_1$, in which $E^{(l)}(\mathcal{P}_{t_p})$ corresponds to the value of the error function $E(\mathcal{P}_{t_p})$ at the lth iteration ($l = 0, 1, 2, \ldots$). At this point, the position of the moving scatterer (object/person) S_M is determined. Then, the overall contribution of the fixed scatterers S_k^F, $k = 0, \ldots, K$, described, here, by the terms $c_{ijF}(f'_q)\exp[j(\vartheta_{ijF}(f'_q))]$, for $i = 1, 2, \ldots, N_R$, $j = 1, 2, \ldots, N_T$, and $q = 0, \ldots, Q-1$, is deduced by subtracting the TVTF $\hat{H}_{ij}(f'_q, t_p)$ from the TVTF $H_{ij}(f'_q, t_p)$ of the channel model.

The estimation process is repeated at any time instant t_p because of the non-stationary behavior of indoor fading channels in the presence of a moving object/person.

V. Numerical Results

In this section, we validate the proposed iterative algorithm to localize the TV position of a single moving person or object (scatterer) in 3D non-stationary indoor environments. This task can be achieved by comparing the exact TV position of the moving scatterer S^M with the estimated TV position. This comparison requires the prior knowledge of the exact TV coordinates of S^M. For an accurate and fair comparison, we will compare the estimates of the TV coordinates $x(t_p)$, $y(t_p)$, and $z(t_p)$ with the corresponding exact values, which are known for test RF signals generated by computer simulations.

The investigated scenario depicted in Fig. 3 considers an indoor area that has a rectangular cuboid shape of length A, width B, and height H equal to 10 m, 5 m, and 2.4 m, respectively. Here, the room is equipped with a 3×3 MIMO communication system. The locations, with respect to the centre of the room, of the fixed omnidirectional transmit and receive antennas A_1^T, A_2^T, A_3^T, A_1^R, A_2^R, and A_3^R were $(-4.9, -2.4, -1.1)$, $(-4.9, -2.4, 1.1)$, $(-4.9, 2.4, 1.1)$, $(4.9, -2.4, -1.1)$, $(4.9, -2.4, 1.1)$, and $(4.9, 2.4, -1.1)$, respectively. For this scenario, the number M_{ij} of fixed objects, which are seen between the jth transmit antenna and ith receive antenna, has been randomly chosen between 5 and 10. Also, the positions of the fixed scatterers have been randomly chosen under the assumption that

$\sum_{k_{ij}=1}^{K_{ij}} c_{k_{ij}}^2 = 1$. The carrier frequency f_0 has been set to 5.9 GHz. The time sampling interval Δt has been chosen to be 0.05 s. The number of sub-carriers Q was fixed to 5 with a frequency sampling period $\Delta f'$ equal to 625 kHz.

As shown in Fig. 3, we consider a single moving person who is modelled by a single point moving scatterer S^M that represents his/her head. The person is assumed to be moving along a straight line. The trajectory $z(t)$ of the moving scatterer S^M is modeled according to [23] as $z(t) = h_{\text{step}} \cos(2\pi f_{\text{step}} t) + h_{\text{head}}$, where the step height h_{step} and the height of the person h_{head} were set to 2,7 cm and 1.7 m, respectively. The walking frequency f_{step} is equivalent to the horizontal speed, which was set to 0.8 m/s (corresponding to a step length of 30 cm). To evaluate the performance of the proposed positioning algorithm, we consider a fall scenario. This allows us to consider three models for the trajectory; sinusoid, linear, and constant. In fact, the fall scenario is comprised of three phases (see Fig. 3). During Phase 1, the person walks with a constant speed for 2.5 s (corresponding to a distance of approximately 2 m). Phase 2 corresponds to the actual fall and starts from the instant the person begins to fall forward until his/her head reaches the floor. Phase 2 lasts 1 s. Finally, Phase 3 lasts 0.5 s, begins when the person's body reaches the floor and stops moving for the rest of the observation time.

Fig. 4 depicts a comparison of the exact vertical displacement $z(t)$ (in m) of the head of the moving person and the corresponding estimated values when employing 3×3 and 2×2 MIMO systems. For the scenario employing a 2×2 MIMO system, we consider the antennas A_1^T, A_2^T, A_1^R, and A_2^R. As can be observed, both system configurations allow an accurate estimation of the TV coordinates of the moving person during the three phases. Moreover, it is clear from Fig. 4, that increasing the number of transmit/receive antennas results in a decrease of the average estimation error. In order to quantify this improvement, we present in Table I the total average estimation error using 3×3 and 2×2 MIMO systems together with the detailed average errors for the different phases of the fall. As can be seen, using a 3×3 (2×2) MIMO system result in an average error of approximately 6 cm (10.5 cm). So, increasing the system dimensions from $N_T = N_R = 2$ to $N_T = N_R = 3$ allows an average precision gain of approximately 5 cm. Note that the total mean estimation error corresponds to the mean square error and was computed by averaging over the observation time (not by averaging over Phases I–III) and is different from the mean error obtained by averaging over the phases. This is because Phase 1 lasts longer than Phase 2 and Phase 3. Furthermore, it can be concluded from Table I that the proposed algorithm behaves better if the point

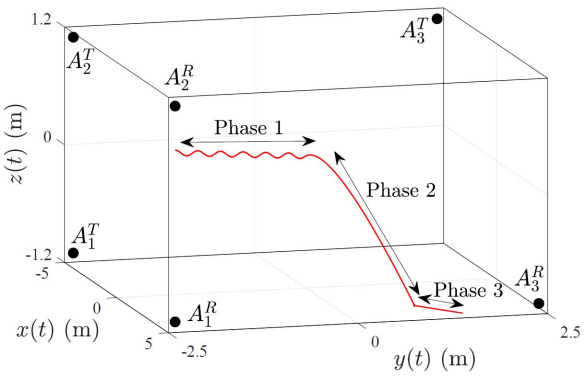

Fig. 3. Scenario description.

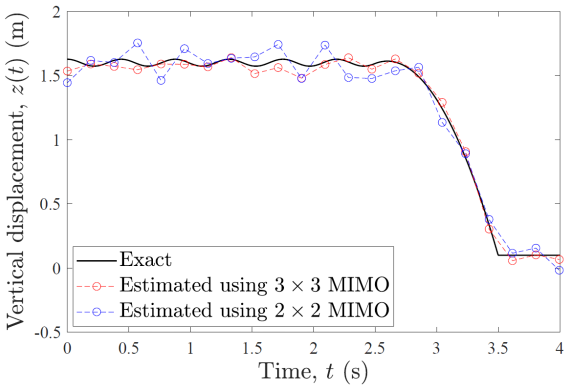

Fig. 4. The exact vertical displacement $z(t)$ (in m) and the corresponding estimated values using 3×3 and 2×2 MIMO systems.

scatterer follows linear trajectories, namely Phase 2 and Phase 3, for which the average error is below 8 cm regardless of the system dimension.

Comparison with existing techniques: For performance assessment purposes, it is of great interest to compare the results of the proposed estimation method with similar existing techniques. For example, estimation algorithms reported in the context of mobile radio communications, e.g., [12]–[16], cannot be considered. This is because the output of such procedures is a vector of channel parameters, such as constant path gains, constant Doppler frequencies, and constant delays, from which it is difficult to extract the TV coordinates of a moving object/person. In addition, these estimators have been proposed under the assumption that the propagation environment can be modelled by a wide-sense stationary channel, where the speed is constant. These results cannot be easily generalized to the case of non-stationary indoor channels. On the other hand, the tech-

TABLE I
MEAN ESTIMATION ERROR

Number of antennas	**Mean error (in cm)**			
	Phase 1	Phase 2	Phase 3	Total
$N_T = N_R = 2$	11.5	7.7	6.5	10.4
$N_T = N_R = 3$	6.3	4.3	3.5	5.8

niques reported in [17] and [18] aim to determine the TV velocity of a moving object/person by exploiting the Doppler characteristics (spectrogram) of the complex channel gain. These procedures assume constant path gains and are based on a linear approximation of the Doppler frequencies. Thus, they cannot be considered for comparison purposes.

VI. Conclusion

This paper proposes a new iterative estimation method to localize a single moving object or person from RF signals in non-stationary indoor areas, which are equipped with a MIMO communication system. First, we have introduced a 3D non-stationary channel model that considers the motion of the object/person (moving scatterer), the presence of fixed objects (fixed scatterers), and the LOS components. The algorithm estimates the TV position of the moving scatterer by fitting the TVTF of the received RF signals as closely as possible to the TVTF of the 3D channel model. The TV coordinates of the moving scatterer are obtained by minimizing the Euclidean norm of the fitting error. The estimate of the TV position of the moving object/person allows the computation of the TV speed, TV path gains, the TV path delays, the TV HAOM, TV VAOM, and the TV Doppler frequencies. A comparison of the exact TV coordinates of the moving scatterer, known from generated test RF signals, with the corresponding estimated values have been presented to confirm the validity of the proposed estimation procedure. Numerical results show that increasing the number of transmit antennas and receive antennas allows a more precise estimation of the TV position of the moving object/person.

Acknowledgement

This work was supported by the WiCare Project funded by the Research Council of Norway under grant number 261895/F20.

References

[1] Infsoft, "Infsoft blog-indoor positioning & more.," Available: https:// www.infsoft.com/blog-en/articleid/53/indoor-positioning-and-indoor-navigation-7-use-cases, 2019. [Online].

[2] A. Yassin et al., "Recent advances in indoor localization: A survey on theoretical approaches and applications," *IEEE Commun. Surveys Tuts.*, vol. 19, no. 2, pp. 1327–1346, 2nd Quart., 2017.

[3] Telit, "The business advantages of a multi-GNSS set-up," Available: https://www.telit.com/blog/multi-gnss-business-advantages/, 2019. [Online].

[4] S. He and S.-H. G. Chan, "Wi-Fi fingerprint-based indoor positioning: Recent advances and comparisons," *IEEE Commun. Surveys Tuts.*, vol. 18, no. 1, pp. 466–490, 1st Quart., 2016.

[5] D. He et al., "3-D spatial spectrum fusion indoor localization algorithm based on CSI-UCA smoothing technique," *IEEE Access*, vol. 6, pp. 59575–59588, 2018.

[6] H. Lee, C. R. Ahn, N. Choi, T. Kim, and H. Lee, "The effects of housing environments on the performance of activity-recognition systems using Wi-Fi channel state information: An exploratory study," *Sensors*, vol. 19, no. 5, pp. 983, 2019.

[7] Y.-L. Sun and Y.-B. Xu, "Error estimation method for matrix correlation-based Wi-Fi indoor localization.," *KSII Trans. Internet Inf. Syst.*, vol. 7, no. 11, pp. 2657–2675, Nov. 2013.

[8] P. Gallo and S. Mangione, "RSS-eye: Human-assisted indoor localization without radio maps," in *IEEE Int. Conf. on Commun. (ICC'15)*, Jun. 2015, pp. 1553–1558.

[9] A. Makki, A. Siddig, M. Saad, J. R. Cavallaro, and C. J. Bleakley, "Indoor localization using 802.11 time differences of arrival," *IEEE Trans. Instrum. Meas.*, vol. 65, no. 3, pp. 614–623, London, UK, Mar. 2016.

[10] T. A. Heya, S. E. Arefin, A. Chakrabarty, and M. Alam, "Image processing based indoor localization system for assisting visually impaired people," in *Ubiquitous Positioning, Indoor Navigation and Location-Based Services (UPINLBS'18)*, Wuhan, China, Dec. 2018, pp. 1–7.

[11] S. Hilsenbeck, D. Bobkov, G. Schroth, R. Huitl, and E. Steinbach, "Graph-based data fusion of pedometer and WiFi measurements for mobile indoor positioning," in *ACM Int. Joint Conf. on Pervasive and Ubiquitous Comput. (UBICOPM'14)*, Seattle, USA, Sept. 2014, pp. 147–158.

[12] R. Schmidt, "Multiple emitter location and signal parameter estimation," *IEEE Trans. Antennas and Propag.*, vol. 34, no. 3, pp. 276–280, Mar. 1986.

[13] A.-J. Van Der Veen, M. C. Vanderveen, and A. Paulraj, "Joint angle and delay estimation using shift-invariance techniques," *IEEE Trans. Signal Processing*, vol. 46, no. 2, pp. 405–418, Feb. 1998.

[14] W. Li, W. Yao, and P. J. Duffett-Smith, "Improving the SAGE algorithm with adaptive partial interference cancellation," in *IEEE 13th Digital Signal Processing Workshop and 5th IEEE Signal Processing Education Workshop (DSP/SPE'09)*, Marco Island, FL, USA, Jan. 2009, pp. 404–409.

[15] D. Umansky and M. Pätzold, "Design of measurement-based wideband mobile radio channel simulators," in *4th Int. Symp. on Wireless Commun. Systems (ISWCS'07)*, Trondheim, Norway, Oct. 2007, pp. 229–235.

[16] A. Fayziyev and M. Pätzold, "The performance of the INLSA in comparison with the ESPRIT and SAGE algorithms," in *Int. Conf. on Advanced Technol. for Commun. (ATC'14)*, Hanoi, Vietnam, Feb. 2014, pp. 332–337.

[17] R. Hicheri, M. Pätzold, and N. Youssef, "Estimation of the velocity of a walking person in indoor environments from mmWave signals," in *IEEE Global Commun. Conf. (GLOBECOM'18)*, Abu Dhabi, UAE, Dec. 2018.

[18] R. Hicheri, M. Pätzold, and N. Youssef, "Estimation of the velocity of a walking person in non-stationary indoor environments from the received RF signal," in *IEEE Latin-American Conf. on Commun. (LATINCOM'18)*, Guadalajara, Mexico, Nov. 2018.

[19] C. Phillips, D. Sicker, and D. Grunwald, "A survey of wireless path loss prediction and coverage mapping methods," *IEEE Commun. Surveys Tuts*, vol. 15, no. 1, pp. 255–270, 1st Quart., 2013.

[20] A. Borhani and M. Pätzold, "A non-stationary channel model for the development of non-wearable radio fall detection systems," *IEEE Trans. Wireless Commun.*, vol. 17, no. 11, pp. 7718–7730, Sept. 2018.

[21] M. Pätzold and C. A. Gutierrez, "Modelling of non-WSSUS channels with time-variant Doppler and delay characteristics," in *IEEE 7th Int. Conf. on Commun. and Electron. (ICCE'18)*, Hue City, Vietnam, Jul. 2018, pp. 1–6.

[22] A. Abdelgawwad and M. Pätzold, "A framework for activity monitoring and fall detection based on the characteristics of indoor channels," in *IEEE 87th Veh. Technol. Conf. (VTC'18-Spring)*, Porto, Portugal, Jun. 2018, pp. 1–7.

[23] S.-U. Jung and Mark S. Nixon, "Estimation of 3D head region using gait motion for surveillance video," in *4th Int. Conf. on Imaging for Crime Detection and Prevention (ICDP'11)*, London, UK, Nov. 2011, pp. 1–6.